SMiRT–12 / K. Kussmaul (Editor)

FG15/4

ANALYSIS OF NON-STEADY ASYMPTOTIC CRACK TIP FIELDS IN POWER LAW CREEPING MATERIALS

D. Linkens[1], D.W. Dean[2] and E.P. Busso[1]

[1]WS Atkins Science and Technology, Epsom, Surrey KT18 5BW, UK
[2]Nuclear Electric plc., Berkeley Technology Centre, Gloucester GL13 9PB, UK

Abstract

Estimates of both transient and steady state values of the $C(t)$-integral for simplified geometries representative of power plant components are compared with results obtained from detailed finite element analyses. Different creep exponents and both primary (mechanical) and secondary (displacement-controlled) loadings are considered.

Estimates of the steady state value C^* were obtained from the EPRI's fully plastic solutions for J-integrals and from Nuclear Electric's R5 high temperature assessment procedure. The results show that, for the deepest cracks considered ($a/w = 0.25$) and $n = 5$, R5 estimates of C^* are conservative by up to 91 % for the full range of geometries analysed. The degree of conservatism increases for $n = 10.4$ and decreases for shallower cracks. The EPRI estimates of C^*, on the other hand, underpredict the numerical solutions by 5 % for $n = 5$, and by 18 % for $n = 10.4$. Bassani's C_t and R5's transient estimates for $C(t)$ were also found in most cases to conservatively predict the finite element results, although some underpredictions were found for the planar geometries shortly after loading. The recommended use of plane stress reference stresses with the R5 procedure, however, provides overall conservatism.

1 Introduction

In a high temperature component whose service life is dominated by creep crack growth, an estimate of the time to failure can be obtained from the knowledge of the time-dependent loading parameter C^* and experimentally determined material data relating it to creep crack growth rates. C^* characterizes both the loading and the geometry of the cracked body and is widely accepted for steady state creep conditions [1,2].

When a constant load is applied to a body, elastic strains develop instantaneously and creep strains gradually start to accumulate close to the crack tip. Small scale creep (SSC) conditions will prevail around the crack tip while the creep zone is small in relation to the crack length. It has been shown that, under these conditions, the stress and strain rate singularities within the creep zone are of the well known HRR fields for power law hardening materials, but the amplitude of the SSC fields exceeds the value of C^*. Therefore, knowledge of a generic energy rate line integral $C(t)$ is needed in order to understand the extent of creep crack growth before the attainment of steady state conditions and thus avoid significant non-conservative predictions.

Although the evaluation of $C(t)$ from finite element solutions is possible, such analyses can be time consuming and costly. The use of simplified estimation formulae in industrial applications involving a broad range of components and crack sizes is therefore essential. Although no widely accepted parameter exists to characterize the amplitude of the singular fields during the transitional regime, several relations have been proposed.

This work reviews the different approaches followed to obtain estimates of $C(t)$, and compares them with results obtained from detailed finite element analyses of simplified geometries representative of power plant components under constant loading. Different creep exponents, crack depths, and both primary (mechanical) and secondary (displacement-controlled) loadings are considered. A more detailed description of this work is given in a companion publication [3].

2 Stress Field Around the Tip of a Stationary Crack

The stress and strain fields around the tip of a stationary sharp crack in a solid obeying power law creep and operating under Mode I conditions can be approximated by the following HRR singularity [1]:

$$\sigma_{ij}(r,\theta,t) = \left[\frac{C(t)}{B\,I_n\,r}\right]^{1/(n+1)} \tilde{\sigma}_{ij}(\theta,n)\,, \tag{1}$$

where θ and r are the polar coordinates from the crack tip, n and B the exponent and material constant from the power law creep relation $\dot{\epsilon}^c = B\,\sigma^n$, and $\tilde{\sigma}_{ij}(\theta,n)$ and I_n are non-dimensional functions which depend on n and have been tabulated by Shih [4].

The magnitude of $C(t)$ depends on time, crack length, material properties and far-field boundary conditions such as load and geometry. For a stationary crack, in the limit when the contour Γ shrinks to the crack tip, it can be expressed as [2]:

$$C(t) = \int_\Gamma \left\{\frac{n}{n+1}\,\sigma_{ij}\,\dot{\epsilon}_{ij}\,dy - \sigma_{ij}\,n_j\,\frac{\partial \dot{u}_i}{\partial x}\,ds\right\}\,, \tag{2}$$

where $\dot{\epsilon}_{ij}$ and $\dot{u}_i$ are the total strain rate and displacement rate respectively, and Γ is a closed path which surrounds the crack tip and encloses a region dominated by creep strains. As time progresses and the load remains constant, the creep zone will extend across the uncracked ligament until creep deformation dominates across the entire body. Thus, as $t \to \infty$, $C(t) \to C^*$, which is independent of the path Γ.

In lieu of the numerical solution of Eq. 2 for SSC, Riedel and Rice [1] proposed an approximate description based on the assumption that the J-integral for elasto-plastic materials is path independent within the creep zone (e.g. very close to the crack tip where the HRR fields are dominant) and equal to K_I^2/E', namely,

$$C(t) = \frac{J}{(n+1)\,t} = \frac{K_I^2}{(n+1)\,t\,E'}\,, \tag{3}$$

where K_I is the Mode I stress intensity factor and $E' = E/(1-\nu^2)$ for plane strain and $E' = E$ for plane stress in terms of the Young's modulus E and Poisson's ratio ν.

Several approximations have been formulated for the intermediate regime between SSC and steady state. Ehlers and Riedel [5] proposed a relation for $C(t)$ based on an interpolation between the SSC solution given by Eq. 3 and the steady state solution:

$$C(t) \simeq C_{ER}(t) = C^* \left\{1 + \frac{t^*}{(n+1)\,t}\right\}\,, \tag{4}$$

where $t^* = K_I^2 / (E' C^*)$ is a characteristic time associated with the transition between SSC and steady state creep.

A different approximation for $C(t)$ was proposed by Ainsworth and Budden [6] using far-field estimates of J. The resulting relation,

$$C(t) \simeq C_{R5}(t) = \frac{J^{n+1}}{n+1} \int_0^t J^n \, dt \,, \tag{5}$$

can be used to obtain estimates of $C(t)$ for various loading conditions, and forms the basis for Nuclear Electric's R5 high temperature assessment procedure. For a constant applied load and with the far field J approximated by $J = K_I^2/E' + C^* t$, Eq. 5 gives

$$C(t) \simeq C_{R5}(t) = C^* \left\{ \frac{[1 + t/t^*]^{n+1}}{[1 + t/t^*]^{n+1} - 1} \right\} . \tag{6}$$

C_{R5} estimates under fixed displacements, needed to predict creep crack growth during stress relaxation of cyclically stabilized materials, are given in Ainsworth and Budden [6].

Bassani et al. [7] proposed an alternative approximation to $C(t)$ based on an analogy to the strain energy release rate interpretation of J and defined as the difference in stress power $(\sigma \, \dot{\epsilon})$ between two equally loaded bodies with incrementally different crack sizes, viz.,

$$C_t(t) = C^* \left\{ \left(\frac{t^*}{(n+1)\, t} \right)^{(n-3)\,/\,(n-1)} + 1 \right\} . \tag{7}$$

It can be shown that, as $t \rightarrow 0$, Eq. 6 correctly tends to the SSC solution of Eq. 4. This limiting behaviour is not however predicted by Eq.7.

Approximations to the steady state parameter C^* can be obtained from either experimental measurements of load and displacement rates [8] or analytically according to (i) EPRI handbook solutions for given creep exponents, load and geometries [9], or to (ii) Nuclear Electric's R5 procedure [10]. The latter uses reference stress techniques to obtain an estimate for C^*, namely

$$C^* \simeq C^*_{R5} = \frac{K_I^2 \; \dot{\epsilon}^c_{ref}}{\sigma_{ref}} \,, \tag{8}$$

where $\dot{\epsilon}^c_{ref}$ is the uniaxial creep strain rate at the reference stress $\sigma_{ref} = \sigma_y \, P / P_{lim}$. Here, P is the applied load, and P_{lim} is the limit load of the structure for a perfectly plastic material of yield strength σ_y.

3 Finite Element Analysis

The finite element code BERSAFE [11] was used to analyse the deformation of three different types of specimens with $a/w = 0.25$: (i) a plane strain single edge cracked plate (ECP), (ii) a plane strain centre cracked plate (CCP), and (iii) an externally circumferentially cracked cylinder (CCC). The specimens were modelled with the finite element meshes shown in Fig. 1 using isoparametric 8-noded elements. The CCC was, in addition, analyzed with $a/w = 0.125$ using the mesh of Fig. 1(b) scaled accordingly. The size of the smallest element in each of the meshes was set at 1/200 of the crack depth. The applied loads were 26 N/width for the ECP and CCP, and 2565 N/circumferential length for the CCC.

The analyses were performed for materials with both low ($n = 5$) and high ($n = 10.4$) creep exponents, with the latter corresponding to a 2.25 Cr - 1 Mo steel at 538 °C [12]. The following material data were used:

Table 1 Material Data

n	B $[s^{-1}\,(MPa)^{-n}]$	E [GPa]	ν
5.0	1.0×10^{-6}	200	0.3
10.4	3.8×10^{-28}	141	0.3

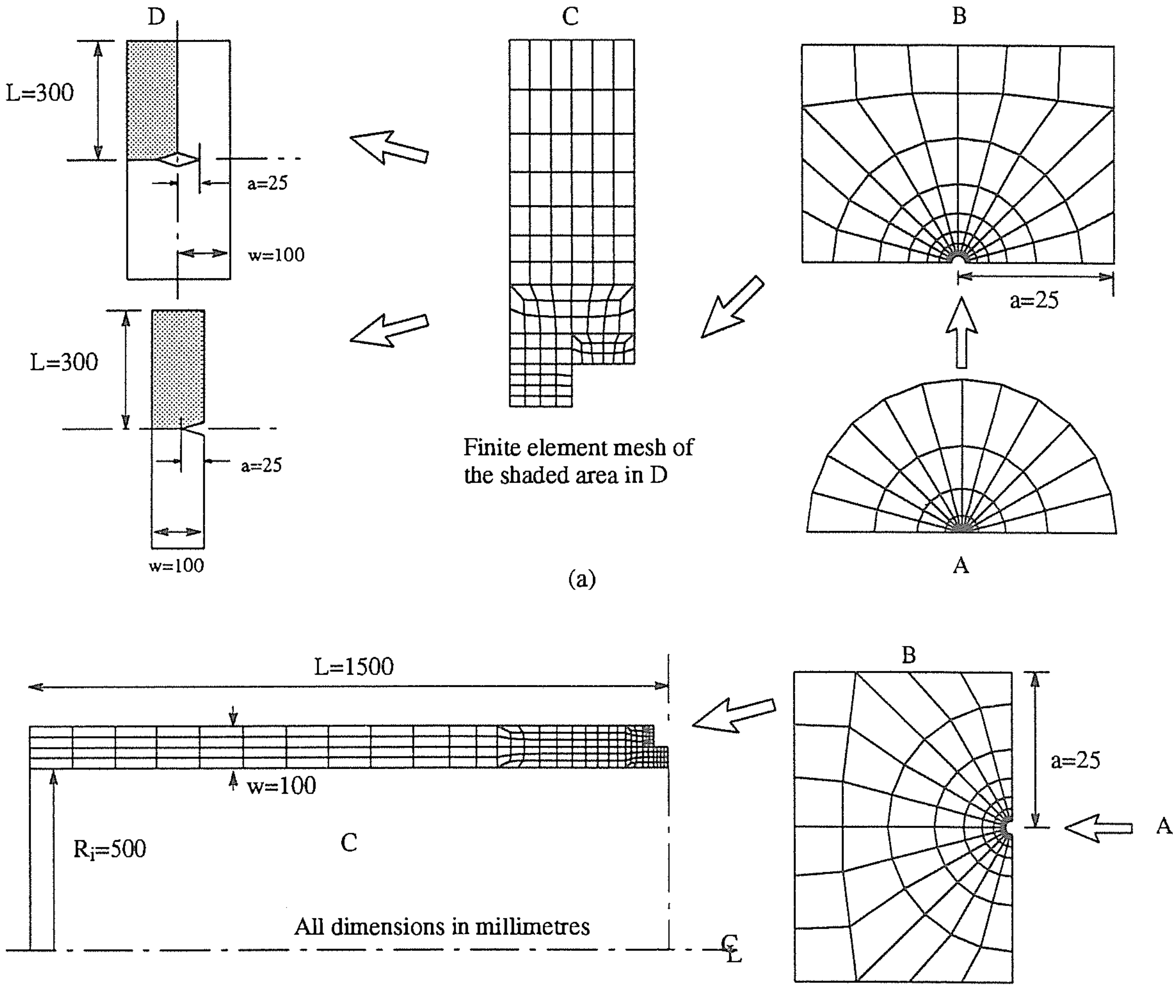

Fig. 1 Finite element models for (a) planar and (b) cylindrical geometries

The numerical values of $C(t)$ were obtained by extrapolating to integration paths Γ of radius $r = 0$ values from integration paths around the crack tip. The path dependency of $C(t)$ was reflected in a variation of up to 3 % from the mean value for $0.03a \leq r \leq 0.8a$. A comparison between Eq. 2's line integrals with values calculated according to the virtual crack extension method revealed them to be within 1 % of each other.

4 Results and Discussion

Figs. 2 (a) and (b) show plots of $C(t)/C^*$ vs. t/t^* for $n = 5$ using C^*_{EPRI} and C^*_{R5} as normalising factors respectively. Finite element results for the different geometries are compared with the C_t and C_{ER} estimates (Eqs. 4 and 7) in Fig. 2(a), and with C_{R5} (Eq.

6) in Fig. 2(b). Similar information is shown in Figs. 3(a) and (b) for $n = 10.4$. The estimates for C_{R5} are based on limit load calculations using plane strain and plane stress assumptions for the planar and cylindrical geometries respectively.

The EPRI estimates of C^* are within 5 % of the numerical solutions for $n = 5$, and within 18 % for $n = 10.4$. As seen in Fig. 3(a), the latter discrepancy originates from the CCC geometry with $a/w = 0.25$. In all cases, the C^*_{EPRI} predictions are under-conservative. Steady state estimates given by R5, on the other hand, are conservative for all the geometries considered. For the deeper cracks ($a/w = 0.25$) with $n = 5$, C^*_{R5} values are conservative by up to 91 % for the range of geometries shown (see Fig. 2(b)). The degree of conservatism increases for $n = 10.4$ and decreases for shallower cracks (e.g. $a/w = 0.125$).

Estimates of the transient behaviour for $n = 5$ show that R5, in most cases, conservatively predicts the finite element values of $C(t)$. At short times, however, underpredictions of up to 20 % were found for the plane strain geometries. For $n = 10.4$, C_{R5} gives a shorter settling time thus underestimating $C(t)$ for $t/t^* \leq 0.9$ for the planar geometries. The recommended use of plane stress reference stresses with R5, however, causes overall conservatism in the procedure, as Fig. 4 reveals for the ECP.

The transient predictions of C_t for $n = 5$, see Fig. 2(a), are 11 % higher than the numerical solutions for $0.7 \leq t/t^* \leq 4$. When n is increased to 10.4, C_t underpredicts the transition time to steady state, even for $t/t^* > 4$ for the CCC in Fig. 3(a). As expected from the form of Eq. 7, C_t approaches C_{ER} at high n.

Fig. 5 shows the values of $C(t)$ for the CCP specimen after the load point displacement was fixed subsequent to the attainment of steady state conditions (at $t/t^* = 4$). The decay of $C(t)$ with time as a result of stress relaxation due to creep is predicted within 15 % by the R5's estimates obtained using a plane strain reference stress approximation with a relation derived from Eq. 5.

Acknowledgments

Permission by Nuclear Electric plc (UK) to publish this work is gratefully acknowledged.

References

[1] Riedel, H. and J.R. Rice (1980), *Fracture Mechanics: Twelfth Conference*, ASTM STP 700, ASTM, Philadelphia, pp. 131-151.

[2] Bassani, J.L. and F.A. McClintock (1981), *Int. Journal Solids Struct.*, V. 17, pp. 479-492.

[3] Busso, E.P., D.W. Dean, and D. Linkens (1993). Submitted for publication.

[4] Shih, C.F. (1983), *Brown University Report MRL E-147*, Providence, RI, USA.

[5] Ehler, R. and H. Riedel (1981), *Advances in Fracture Research,* Proc. Fifth Int. Conf. on Fracture, Cannes, D. Francois (ed.), Vol. 2, Pergamon press, NY, pp. 691-698.

[6] Ainsworth, R.A. and P.J. Budden (1988), *CEGB Report RD/B/6005/R88.*

[7] Bassani, J.L., D.E. Hawk, and A. Saxena (1989), *Non-linear Fracture Mechanics, ASTM* STP 995, A. Saxena et al. eds., ASTM, Philadelphia, pp. 7-26.

[8] Landes, J.D. and J.A. Begley (1976), *Mechanics of Crack Growth*, ASTM STP 590, ASTM, Philadelphia, PA, pp. 128-148.

[9] Kumar V., et al., *EPRI NP-1931 (1981), EPRI RP 1237-1*, 5th and 6th Report (March 1982), *Final Report NP-3607* (Aug. 1984), Elect. Power Res. Inst., Palo Alto, CA.

[10] Ainsworth, R.A., G.G. Chell, M.C. Coleman, I.W. Goodall, D.J. Gooch, J.R. Haigh, S.T. Kimmins, and G.J. Neate (1987), *Fat. Fract. Engng. Mater. Struct.*, V. 10(2), pp. 115-127.

[11] BERSAFE 1988 User's Guide, *CEGB*, Berkeley, United Kingdom.

[12] Logsdon, W.A., P.K. Liaw, and A. Saxena (1986), *Engng. Fract. Mech.*, V. 25(3), p. 259.

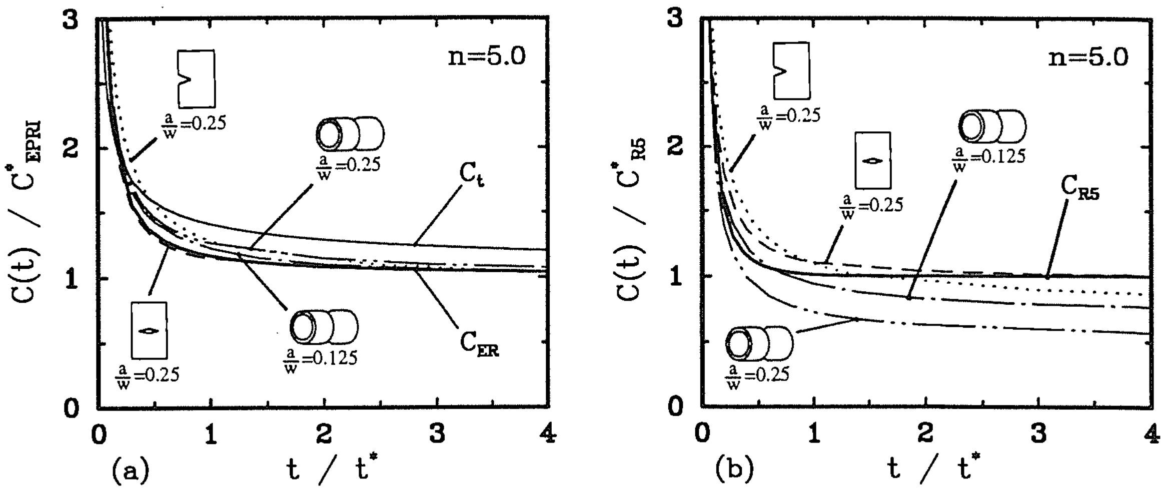

Fig. 2 Comparison of the finite element results with analytical estimates of $C(t)$ for $n = 5.0$: (a) C_t and C_{ER} normalised by EPRI's steady state estimate, and (b) C_{R5} normalised by C^*_{R5}

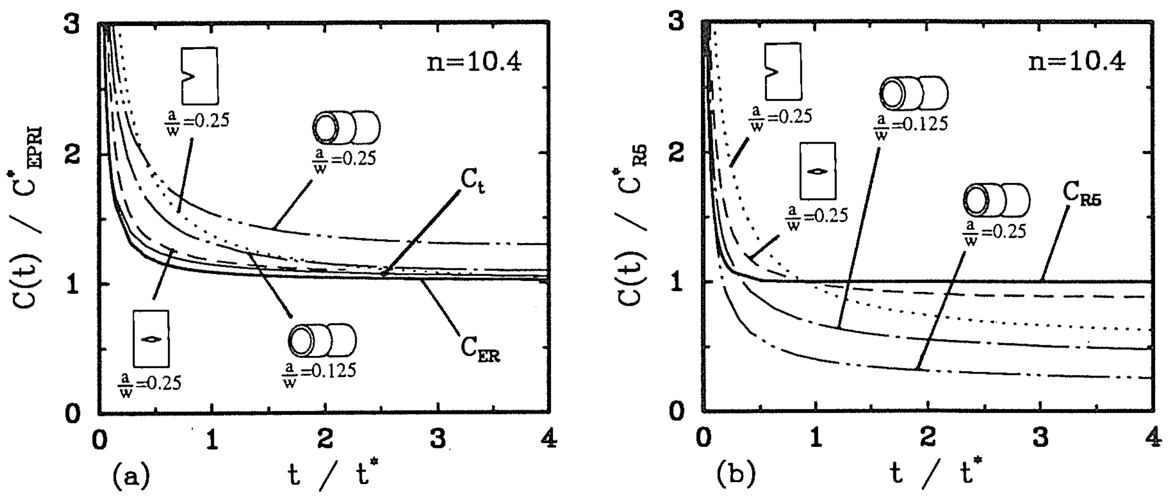

Fig. 3 Comparison of the finite element results with analytical estimates of $C(t)$ for $n = 10.4$: (a) C_t and C_{ER} normalised by EPRI's steady state estimate, and (b) C_{R5} normalised by C^*_{R5}

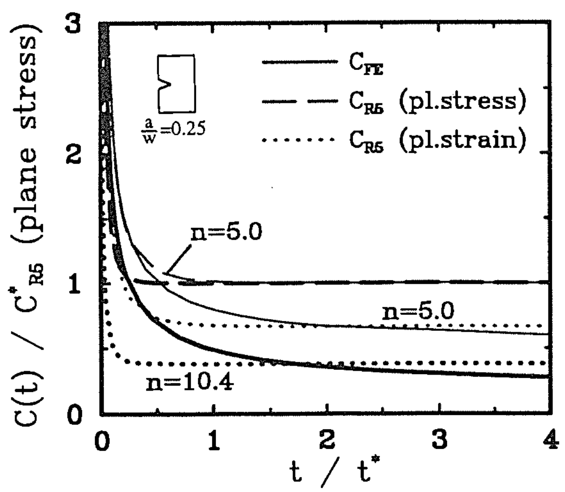

Fig. 4 C_{R5} estimates using both plane stress and plane strain reference stress assumptions

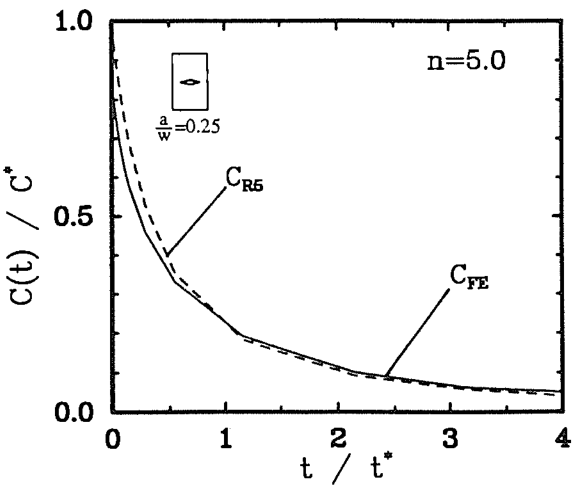

Fig. 5 Variation of $C(t)$ under fixed load point displacements